

# Inhibition of Recombinant N-Type $\text{Ca}_V$ Channels by the $\gamma_2$ Subunit Involves Unfolded Protein Response (UPR)-Dependent and UPR-Independent Mechanisms

Alejandro Sandoval,<sup>1,3</sup> Arturo Andrade,<sup>1</sup> Aaron M. Beedle,<sup>4</sup> Kevin P. Campbell,<sup>4</sup> and Ricardo Felix<sup>2</sup>

Departments of <sup>1</sup>Physiology, Biophysics, and Neuroscience, and <sup>2</sup>Cell Biology, Center for Research and Advanced Studies of the National Polytechnic Institute, Mexico City, 07300, Mexico, <sup>3</sup>School of Medicine Faculty of Superior Studies Iztacala, National Autonomous University of Mexico, Tlalnepantla, 54090, Mexico, and <sup>4</sup>Howard Hughes Medical Institute and Department of Molecular Physiology and Biophysics, University of Iowa Roy J. and Lucille A. Carver College of Medicine, Iowa City, Iowa 52242-1101

Auxiliary  $\gamma$  subunits are an important component of high-voltage-activated calcium ( $\text{Ca}_V$ ) channels, but their precise regulatory role remains to be determined. In the current report, we have used complementary approaches including molecular biology and electrophysiology to investigate the influence of the  $\gamma$  subunits on neuronal  $\text{Ca}_V$  channel activity and expression. We found that coexpression of  $\gamma_2$  or  $\gamma_3$  subunits drastically inhibited macroscopic currents through recombinant N-type channels ( $\text{Ca}_V2.2/\beta_3/\alpha_2\delta$ ) in HEK-293 cells. Using inhibitors of internalization, we found that removal of functional channels from the plasma membrane is an improbable mechanism of current regulation by  $\gamma$ . Instead, changes in current amplitude could be attributed to two distinct mechanisms. First,  $\gamma$  subunit expression altered the voltage dependence of channel activity. Second,  $\gamma$  subunit expression reduced N-type channel synthesis via activation of the endoplasmic reticulum unfolded protein response. Together, our findings (1) corroborate that neuronal  $\gamma$  subunits significantly downregulate  $\text{Ca}_V2.2$  channel activity, (2) uncover a role for the  $\gamma_2$  subunit in  $\text{Ca}_V2.2$  channel expression through early components of the biosynthetic pathway, and (3) suggest that, under certain conditions, channel protein misfolding could be induced by interactions with the  $\gamma$  subunits, supporting the notion that  $\text{Ca}_V$  channels constitute a class of difficult-to-fold proteins.

**Key words:**  $\text{Ca}^{2+}$  channels;  $\gamma$  subunit; genistein; HEK-293 cells; PERK; UPR

## Introduction

Voltage-activated  $\text{Ca}^{2+}$  ( $\text{Ca}_V$ ) channels are essential for basic neurophysiological processes including transmitter release, signal transduction, and gene expression (Berridge, 1998; Hille, 2001).  $\text{Ca}_V$  channels may be broadly divided into low-voltage-activated (LVA) (T-type) and high-voltage-activated (HVA) channels (types L, N, P, Q, and R), with this classification indicative of their functional and pharmacological properties (Hille, 2001; Catterall et al., 2005). At the molecular level, it has been reported that as many as four subunits may form the  $\text{Ca}_V$  channel complex (Catterall et al., 2005; Felix, 2005). The  $\text{Ca}_V\alpha_1$  subunit is

the ion-conducting element and contains the gating and voltage sensor machinery of the channel. The  $\text{Ca}_V\beta$  subunit is entirely cytoplasmic and participates in a wide range of regulatory actions. The  $\text{Ca}_V\alpha_2\delta$  consist of an extracellular  $\alpha_2$  peptide linked by disulfide bonds to a transmembrane  $\delta$  domain, and is responsible for diverse regulatory actions on the membrane expression and functional activity of the pore-forming subunit. Lastly, the transmembrane  $\text{Ca}_V\gamma$  subunit has been found in skeletal muscle  $\text{Ca}_V$  channels, and related subunits are expressed in heart and brain. The effects of the neuronal  $\text{Ca}_V\gamma$  subunit on  $\text{Ca}^{2+}$  channels have been studied in heterologous systems, and although some of the results are discordant, the consensus seems to be that  $\text{Ca}_V\gamma$  downregulates channel activity (Black, 2003; Kang and Campbell, 2003).

The  $\text{Ca}_V\gamma$  family comprises eight tetraspan membrane glycoproteins with intracellular N and C termini (Black, 2003; Kang and Campbell, 2003). One of the most versatile members of this family of proteins is the neuronal  $\text{Ca}_V\gamma_2$  subunit. Recent studies have shown that, in addition to its role as a component of  $\text{Ca}^{2+}$  channels,  $\text{Ca}_V\gamma_2$  also serves as a chaperone for synaptic targeting of the AMPA receptor (Qiao and Meng, 2003; Letts, 2005) and can act as a cell adhesion molecule (Price et al., 2005). In addition, there has been some controversy about the function of the neuronal  $\text{Ca}_V\gamma$ s (including  $\text{Ca}_V\gamma_2$ ) as voltage-gated  $\text{Ca}^{2+}$  channel subunits (Moss et al., 2003), because their functional effects are

Received Oct. 20, 2006; revised Feb. 15, 2007; accepted Feb. 16, 2007.

This work was supported by grants from the National Council for Science and Technology (Conacyt) and the Miguel Aleman Foundation (R.F.). Doctoral fellowships from Conacyt to A.S. and A.A. are gratefully acknowledged. K.P.C. is an Investigator of the Howard Hughes Medical Institute. We gratefully appreciate the technical expertise of B. E. Reyes, L. Escobedo, M. Oliva, M. Urban, and G. Aguilar. We also thank M. Oyadomari and D. Ron (Skirball Institute of Biomolecular Medicine, New York, NY), who generously provided the PERK cDNA constructs, as well as L. M. Alvarez-Salas (Center for Research and Advanced Studies of the National Polytechnic Institute, Mexico City, Mexico) for the pEGFP-C1 vector, J. C. Gomora (Institute of Cellular Physiology—National Autonomous University of Mexico, Mexico City, Mexico) for the  $\text{Ca}_V3.2$  channel stably expressing HEK-293 cell line, and A. Almanza for helpful advice on the DRG neuron culture.

Correspondence should be addressed to Dr. Ricardo Felix, Departamento de Biología Celular, Centro de Investigación y de Estudios Avanzados del Instituto Politécnico Nacional, Avenida Instituto Politécnico Nacional #2508, Colonia Zacatenco, México D.F., CP 07300, México. E-mail: rfelix@fisio.cinvestav.mx.

DOI:10.1523/JNEUROSCI.4566-06.2007

Copyright © 2007 Society for Neuroscience 0270-6474/07/273317-11\$15.00/0

relatively small in certain model systems. However, diverse studies agree that Ca<sub>v</sub> $\gamma$ <sub>2</sub> inhibits Ca<sup>2+</sup> current. Electrophysiological recordings have shown that Ca<sub>v</sub> $\gamma$ <sub>2</sub> increases steady-state inactivation of neuronal Ca<sub>v</sub>2.1 (P/Q-type) channels (Letts et al., 1998; Klugbauer et al., 2000; Rousset et al., 2001) and induces a significant decrease in the current amplitude through Ca<sub>v</sub>2.2 (N-type) channels expressed in *Xenopus* oocytes (Kang et al., 2001).

In the current report, we show that the coexpression of neuronal Ca<sub>v</sub> $\gamma$ <sub>2</sub> or Ca<sub>v</sub> $\gamma$ <sub>3</sub> subunits substantially reduces whole-cell currents through recombinant Ca<sub>v</sub>2.2 channels heterologously expressed in human embryonic kidney 293 (HEK-293) cells. Our data suggest that current inhibition may involve important alterations in the functional properties of the Ca<sub>v</sub>2.2 channels as well as activate the unfolded protein response (UPR) to suppress channel translation.

## Materials and Methods

**Materials.** Chloroquine (catalog #C-6628) and genistein (catalog #G-6649) were obtained from Sigma (St. Louis, MO); benzyloxycarbonylleucyl-norleucinal (calpeptin; catalog #03-34-0051) and carbobenzoxy-L-leucyl-L-leucyl-L-leucinal (MG-132) (catalog #03-34-0051) were from Calbiochem (La Jolla, CA). N-[N-(L-3-*trans*-Carboxirane-2-carbonyl)-L-leucyl]-agmatine (E-64) (catalog #10874523001) was purchased from Roche (Basel, Switzerland), and DMSO (catalog #RES2166D) was from Research Organics (Cleveland, OH). All other chemicals were of reagent grade and obtained from different commercial sources.

**cDNA clones.** Cell expression constructs were made by standard techniques, and their fidelity was verified by DNA sequencing. The  $\alpha$ <sub>1B</sub>-pKCRH2 construct containing the cDNA clone encoding the rabbit brain N-type Ca<sup>2+</sup> channel Ca<sub>v</sub>2.2 pore-forming subunit (formerly  $\alpha$ <sub>1B</sub>; GenBank accession number D14157) (Fujita et al., 1993) was kindly provided by B. Adams (Utah State University, Logan, UT). The cDNA coding the rat brain Ca<sub>v</sub> $\alpha$ <sub>2</sub> $\delta$ -1 (M86621) (Kim et al., 1992), rat brain Ca<sub>v</sub> $\beta$ <sub>3</sub> (M88751) (Castellano et al., 1993), mouse brain Ca<sub>v</sub> $\gamma$ <sub>2</sub> subunit (NM\_007583) (Letts et al., 1998), and human skeletal muscle sarcosin (AF016028) (Crosbie et al., 1997) were subcloned into the pcDNA3 vector (Invitrogen, Carlsbad, CA). The mouse brain Ca<sub>v</sub> $\gamma$ <sub>3</sub> (NM\_019430) (Letts et al., 2005) cDNA was subcloned into the pIRES-hrGFP1a vector (Stratagene, La Jolla, CA).

The Ca<sub>v</sub>2.2 cDNA was inserted into the pEGFP-C1 vector (Clontech, Mountain View, CA) downstream and in-frame with the enhanced fluorescent green protein (EGFP) to generate the EGFP-Ca<sub>v</sub>2.2 construct. The Ca<sub>v</sub> $\gamma$ <sub>2</sub> subunit was excised from the pcDNA3 vector using *Hind*III and *Bam*HI and subcloned into the *Hind*III/*Bam*HI sites of the pAd5CMVκ-NpA shuttle vector as described previously (Arikath et al., 2003). This construct was used as a template to generate the Ca<sub>v</sub> $\gamma$ <sub>2</sub> N48Q mutant (see below).

The PKR-like endoplasmic reticulum (ER)-associated kinase (PERK) wild-type (PERK.WT.9E10.pCDNA.amp) and mutant constructs (PERK.K618A.9E10.pCDNA.amp; PERK.dC.9E10.pCDNA.amp) cloned into the *Eco*RI/*Xho*I sites of the expression vector pcDNAI/Amp (Invitrogen) (Harding et al., 1999) were kindly provided by M. Oyadomari and D. Ron (Skirball Institute of Biomolecular Medicine, New York, NY).

**Site-directed mutagenesis.** An asparagine-to-glutamine substitution at position 48 from the amino terminus of the Ca<sub>v</sub> $\gamma$ <sub>2</sub> subunit was introduced to prevent N-linked glycosylation. This point mutation was introduced with ~40-mer synthetic oligonucleotides using the QuikChange XL mutagenesis kit (Stratagene). The cDNA of the mutant Ca<sub>v</sub> $\gamma$ <sub>2</sub> channel subunit was sequenced on an automated Sequencer (ABI Prism 310; PerkinElmer Applied Biosystems, Norwalk, CT).

**Cell culture and transfection.** HEK-293 cells (American Type Culture Collection, Manassas, VA) were grown in DMEM-high glucose supplemented with 10% horse serum, 2 mM L-glutamine, 110 mg/L sodium pyruvate, 100 U/ml penicillin, and 100  $\mu$ g/ml streptomycin at 37°C in a 5% CO<sub>2</sub>/95% air humidified atmosphere. After splitting the cells on the previous day and seeding at ~60% confluency, cells were transfected using the Lipofectamine Plus reagent (Invitrogen) with the cDNA clones

mentioned previously, according to the manufacturer's instructions. All Ca<sub>v</sub> channel subunits were transfected at the same time.

The human embryonic kidney cells (HEK-293 cells) stably expressing the Ca<sub>v</sub>3.2 channel (GenBank accession number AF051946) (Cribbs et al., 1998) were grown as described previously (Avila et al., 2006). For electrophysiological recordings, cells were lifted off plates, reseeded on poly-L-lysine (0.05%)-precoated glass coverslips and used 2–6 h after plating.

Single dorsal root ganglion (DRG) neurons were isolated from 7- to 9-d-old BALB/c mice as described previously (Salceda et al., 2006) with slight modifications. In short, a dorsal laminectomy was performed and DRGs with the corresponding spinal roots were dissected out. After dissection, the ganglia were incubated with 1.25 mg/ml collagenase type IV and trypsin (Sigma), in DMEM culture medium at 37°C for 30 min. Thereafter, cells were dissociated by repeated pipetting. Dissociated DRG neurons were resuspended in DMEM supplemented with 10% fetal bovine serum, 100 U/ml penicillin, and 100  $\mu$ g/ml streptomycin. Cells were plated on poly-L-lysine (0.05%)-precoated glass coverslips placed into 35 mm culture plates, and 24 h later were transfected with the Ca<sub>v</sub> $\gamma$ <sub>2</sub> subunit cDNA subcloned into the pAd5CMVκ-NpA shuttle vector using the Fugene transfection reagent (Roche Molecular Biochemicals, Indianapolis, IN). Forty-eight hours after transfection, DRG neurons were subjected to electrophysiological recording.

**Electrophysiology.** Ba<sup>2+</sup> currents through recombinant N-type Ca<sup>2+</sup> channels heterologously expressed in HEK-293 were recorded as described previously (Sandoval et al., 2004) using the whole-cell configuration of the patch-clamp technique (Marty and Neher, 1995). All experiments were performed at room temperature (RT) (~22°C) and a holding potential (HP) of –80 mV. Currents were recorded with an Axopatch 200B amplifier (Molecular Devices, Union City, CA) and filtered at 2 kHz (internal four-pole Bessel filter). Currents were digitized at 5.71 kHz, using a DigiData 1320A interface (Molecular Devices) and analyzed using the pCLAMP (Molecular Devices) and SigmaPlot (Systat Software, Richmond, CA) software. Linear capacitive currents were minimized via the capacitive transient cancellation feature of the amplifier. The remaining linear components were subtracted using a P/4 protocol. Membrane capacitance was determined as described previously (Avila et al., 2004) and used to normalize currents. The bath recording solution contained the following (in mM): 10 BaCl<sub>2</sub>, 125 TEA-Cl, 10 HEPES, and 15 glucose, pH 7.3. The internal solution consisted of the following (in mM): 110 CsCl, 5 MgCl<sub>2</sub>, 10 EGTA, 10 HEPES, 4 Na-ATP, and 0.1 Na-GTP, pH 7.3. Whole-cell patch-clamp endogenous K<sup>+</sup> currents were obtained from an HP of –80 mV applying test pulses every 20 s as described previously (Avila et al., 2004). Current signals were filtered at 2 kHz and digitized at 5.71 kHz. Recording solutions mainly consisted of the following (in mM): 140 NaCl, 3 KCl, 5 CaCl<sub>2</sub> (external solution) and 130 K-Asp, and 8 KCl (internal solution).

**Flow cytometry.** Untransfected and Ca<sub>v</sub> channel subunit-expressing HEK-293 cells were kept in culture for 48 h as described previously. Cells were dispersed by treatment with PBS/trypsin (0.05%) and harvested in PBS at RT. The dispersed cells were washed with PBS plus 2% EDTA (PBS/EDTA) and pelleted by low-speed centrifugation. Cells were resuspended in PBS/EDTA (400  $\mu$ l aliquots). Cell-associated fluorescence was measured using a FACScan flow cytometer (Becton Dickinson, Mountain View, CA) in two different assays. In the first series of experiments, cytometric analysis was performed directly in HEK-293 cells expressing the EGFP-Ca<sub>v</sub>2.2 fusion protein using an excitation wavelength of 488 nm and an emission wavelength of 508 nm. In the second series of experiments, performed in HEK-293 cells expressing Ca<sub>v</sub>2.2 channels (transfected in the pKCRH2 vector), an affinity-purified anti-Ca<sub>v</sub> $\alpha$ <sub>2</sub> primary antibody (GP1) was used in a 1:1000 dilution. The rabbit anti-guinea pig secondary antibody (Zymed, San Francisco, CA) was conjugated with FITC. In this case, cells were first incubated with the antibodies raised against the extracellular Ca<sub>v</sub> $\alpha$ <sub>2</sub> subunit for 30 min at RT, and then with the secondary antibody for additional 30 min at RT. Fluorescence was assayed using an excitation wavelength of 488 nm and an emission wavelength of 525 nm.

**Statistical analysis.** Curve fitting and statistical analyses were performed using the SigmaPlot 8.0 software package (SPSS, Chicago, IL).

The significance of observed differences was evaluated by nonpaired Student's *t* test. A value of *p* < 0.05 was considered to be significant.

## Results

### Heterologous expression of Ca<sub>v</sub> $\gamma$ <sub>2</sub> specifically inhibits I<sub>Ba</sub> through recombinant Ca<sub>v</sub>2.2 channels

To examine the effects of Ca<sub>v</sub> $\gamma$ <sub>2</sub> on neuronal Ca<sup>2+</sup> channels, this regulatory subunit was cotransfected with N-type channels (Ca<sub>v</sub>2.2/ $\beta$ <sub>3</sub>/ $\alpha$ <sub>2</sub> $\delta$ ) in HEK-293 cells 48 h before current recordings. Representative traces of Ba<sup>2+</sup> current (I<sub>Ba</sub>) evoked by test pulses to +10 mV recorded from control (without Ca<sub>v</sub> $\gamma$ <sub>2</sub>) and cells expressing Ca<sub>v</sub> $\gamma$ <sub>2</sub> are depicted in Figure 1A. Coexpression of Ca<sub>v</sub> $\gamma$ <sub>2</sub> decreased I<sub>Ba</sub> amplitude through N-type channels to nearly undetectable levels. Given the drastic effect of Ca<sub>v</sub> $\gamma$ <sub>2</sub>, it was necessary to rule out any potential interference of the pAd5CMVK-NpA construct with the transcriptional machinery of the cells; therefore, we generated a pIRES plasmid construct encoding the related Ca<sub>v</sub> $\gamma$ <sub>3</sub> sequence (~66% amino acid identity to mouse Ca<sub>v</sub> $\gamma$ <sub>2</sub>) (Letts et al., 2003) and examined its actions using the same approach. Expression of the Ca<sub>v</sub> $\gamma$ <sub>3</sub> construct also resulted in a near complete loss of current amplitude (Fig. 1A, B).

Expression of SS (sarcospan), an unrelated tetraspan protein, with N-type channels had no effect on I<sub>Ba</sub>, suggesting a specific functional interaction of Ca<sub>v</sub> $\gamma$ s with the channel complex (Fig. 1A, B). Likewise, Ca<sub>v</sub> $\gamma$  regulation was specific for high-voltage-activated Ca<sup>2+</sup> channels as Ca<sub>v</sub> $\gamma$  expression had no effect on endogenous K<sup>+</sup> currents (Fig. 1C), nor recombinant low-voltage-activated Ca<sub>v</sub>3.2 (T-type) currents (Fig. 1D).

To confirm that current inhibition by the Ca<sub>v</sub> $\gamma$  subunits was not simply a nonspecific effect of overexpression, we next transfected HEK-293 cells using different concentrations of cDNAs. As we discuss later, this also allowed us to obtain currents large enough for accurate analysis. Hence, we fixed the cDNA concentration for Ca<sub>v</sub>2.2,  $\beta$ <sub>3</sub>, and  $\alpha$ <sub>2</sub> $\delta$  subunit transfection (1:1:1 molar ratio) and varied the Ca<sub>v</sub> $\gamma$ <sub>2</sub> concentrations. Our results show that, on coexpression of the Ca<sub>v</sub> $\gamma$ <sub>2</sub> cDNA in molar ratios ranging from 1:0.1 to 1:1.4 (with respect to the other Ca<sub>v</sub> channel subunits), the amplitude of I<sub>Ba</sub> through Ca<sub>v</sub>2.2/ $\beta$ <sub>3</sub>/ $\alpha$ <sub>2</sub> $\delta$  channels decreased significantly as the relative molar ratio of Ca<sub>v</sub> $\gamma$ <sub>2</sub> increased (Fig. 2A). These data suggested a Ca<sub>v</sub> $\gamma$ <sub>2</sub>-specific inhibitory effect. As shown in Figure 2B, current regulation was observed at virtually all voltages tested.

### Regulation of whole-cell conductance and channel steady-state inactivation by the Ca<sub>v</sub> $\gamma$ <sub>2</sub> subunit

Because the gating of Ca<sub>v</sub>2.2 channels is influenced by the coexpression of auxiliary subunits, the reduction in I<sub>Ba</sub> may reflect a Ca<sub>v</sub> $\gamma$ <sub>2</sub>-mediated effect on the voltage dependence of channel activity. To test this, we constructed activation and steady-state inactivation curves from analysis of macroscopic currents. Increasing Ca<sub>v</sub> $\gamma$ <sub>2</sub> molar ratio clearly decreases the functional expression of recombinant Ca<sub>v</sub>2.2-containing channels in a dose-dependent manner as shown by a significant decrease in macroscopic conductance (Fig. 3A). There was a significant shift in the half-maximal voltage (*V*<sub>1/2</sub>) of the *G*-*V* curves in the presence of increasing concentrations of Ca<sub>v</sub> $\gamma$ <sub>2</sub>, consistent with the idea that this auxiliary subunit affects the voltage sensitivity of Ca<sub>v</sub>2.2 channels (Fig. 3B).

The voltage dependence of steady-state inactivation was also significantly affected by the presence of the Ca<sub>v</sub> $\gamma$ <sub>2</sub> subunit. As shown in Figure 4, there is a significant >10 mV hyperpolarizing shift in the Ca<sub>v</sub>2.2 steady-state inactivation curve on coexpression with increasing molar ratios of the Ca<sub>v</sub> $\gamma$ <sub>2</sub> subunit.

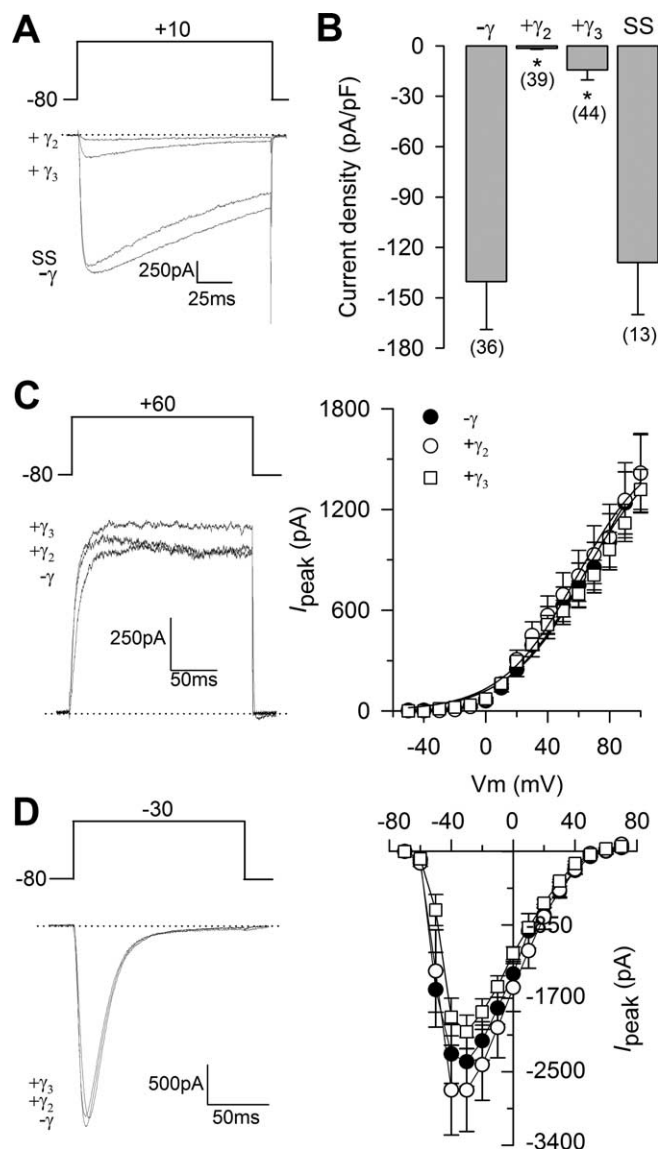


**Figure 1.** The Ca<sub>v</sub> $\gamma$ <sub>2</sub> and Ca<sub>v</sub> $\gamma$ <sub>3</sub> auxiliary subunits specifically inhibit current through Ca<sub>v</sub>2.2/Ca<sub>v</sub> $\alpha$ <sub>2</sub> $\delta$ /Ca<sub>v</sub> $\beta$ <sub>3</sub> channels heterologously expressed in HEK-293 cells. **A**, Representative current traces from control cells (- $\gamma$ ) or cells coexpressing either the Ca<sub>v</sub> $\gamma$ <sub>2</sub> or Ca<sub>v</sub> $\gamma$ <sub>3</sub> subunits or the 4TM protein sarcospan (SS). Currents were elicited by voltage steps to +10 mV from a holding potential of -80 mV. **B**, Comparison of I<sub>Ba</sub> density in individual HEK-293 cells determined as the current amplitude at V<sub>m</sub> of +10 mV normalized by cell capacitance (picoamperes per picofarad). The number of tested cells is listed in parentheses. **C**, Left, Representative traces of endogenous macroscopic K<sup>+</sup> currents elicited by step changes in membrane potential from -80 to +60 mV in untransfected HEK-293 cells (- $\gamma$ ) or cells expressing the Ca<sub>v</sub> $\gamma$  subunits. Right, Relationship between I<sub>Ba</sub> [measured at its maximum amplitude after the step change in membrane potential (V<sub>m</sub>)] from a holding potential of -80 mV and membrane voltage in control (n = 10) and Ca<sub>v</sub> $\gamma$ -expressing cells (n = 10). **D**, Left, Representative traces of macroscopic currents through low-threshold channels of the Ca<sub>v</sub>3.2 class. Currents were recorded from HEK-293 cells stably expressing Ca<sub>v</sub>3.2 channels in the absence (- $\gamma$ ) or presence of the Ca<sub>v</sub> $\gamma$  subunits in response to depolarizing steps to -30 mV. Right, Averaged peak currents plotted against the test potential under the indicated experimental conditions. Currents were activated from a holding potential of -80 mV by voltage steps applied at 0.05 Hz to various test potentials between -70 and +70 mV (n = 10–18). The asterisks denote significant differences (*p* < 0.05) compared with control. Error bars indicate SEM.

### Regulation of Ca<sub>v</sub>2.2 channel currents by Ca<sub>v</sub> $\gamma$ in the absence of Ca<sub>v</sub> $\alpha$ <sub>2</sub> $\delta$ and Ca<sub>v</sub> $\beta$ subunits

Previous studies examining the influence of auxiliary Ca<sub>v</sub> $\alpha$ <sub>2</sub> $\delta$  and Ca<sub>v</sub> $\beta$  subunits on the inhibitory actions of the neuronal Ca<sub>v</sub> $\gamma$

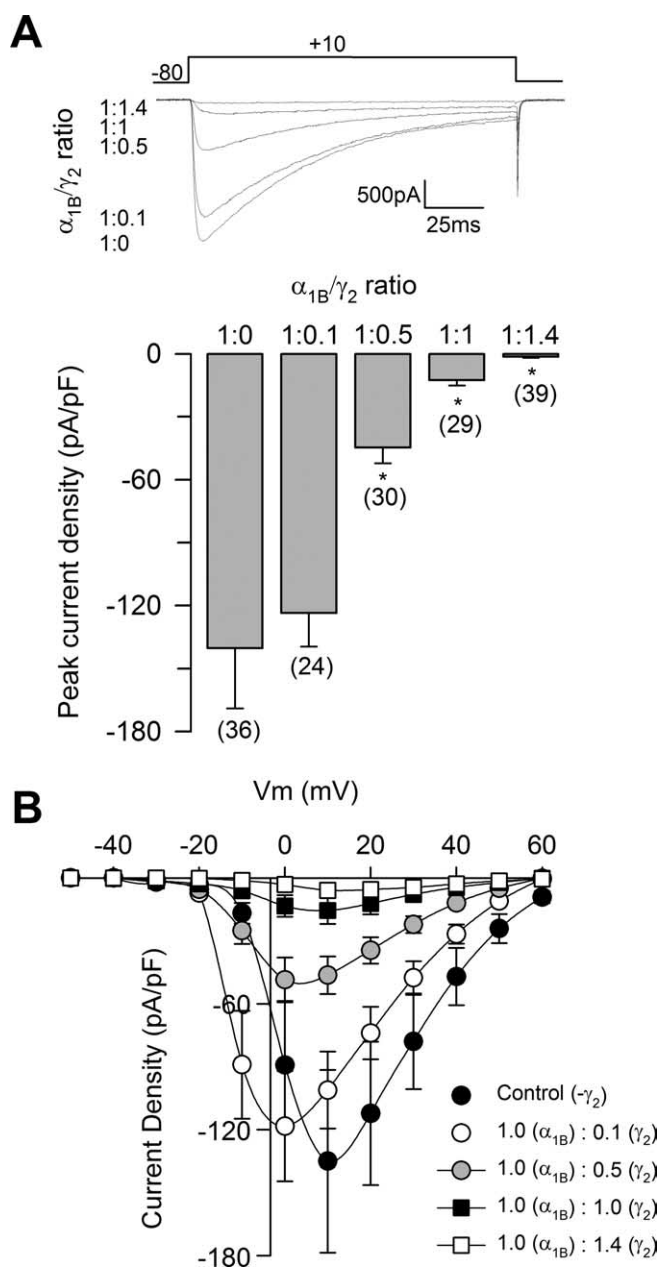


**Figure 2.** The Ca<sub>v</sub> $\gamma_2$  subunit inhibits recombinant N-type Ca<sup>2+</sup> channels in a concentration-dependent manner. **A**, Representative Ba<sup>2+</sup> currents recorded (top) and comparison of averaged peak current density (bottom) in HEK-293 cells expressing Ca<sub>v</sub>2.2( $\alpha_{1B}$ )/Ca<sub>v</sub> $\alpha_2\delta$ /Ca<sub>v</sub> $\beta_3$  channels. Currents were elicited by depolarizing pulses to +10 mV from a holding potential of -80 mV, in the absence (1:0) and the presence of different concentrations of Ca<sub>v</sub> $\gamma_2$  cDNA in the transfection mixture. **B**, I-V relationships for peak *I*<sub>ba</sub> density through Ca<sub>v</sub>2.2/Ca<sub>v</sub> $\alpha_2\delta$ /Ca<sub>v</sub> $\beta_3$  channels in control cells ( $-\gamma_2$ ) and cells coexpressing the Ca<sub>v</sub> $\gamma_2$  cDNA in molar ratios ranging from 1:0.1 to 1:1.4 in relation to the Ca<sub>v</sub>2.2 subunit (*n* = 12–14). Error bars indicate SEM, and the asterisks denote significant differences (*p* < 0.05) compared with control.

subunits have given contrasting results. Hence, although it has been reported that the Ca<sub>v</sub> $\gamma_2$ -induced current inhibition is more pronounced with Ca<sub>v</sub> $\alpha_2\delta$  expression (Kang et al., 2001), the Ca<sub>v</sub> $\gamma_7$  subunit inhibitory actions seem not to be dependent on the presence of the Ca<sub>v</sub> $\alpha_2\delta$  subunit as part of the N-type channel complex (Moss et al., 2002). Therefore, we next tested the role of other Ca<sup>2+</sup> channel regulatory subunits on Ca<sub>v</sub> $\gamma$  inhibition. To evaluate this, HEK-293 cells were cotransfected with Ca<sub>v</sub>2.2/ $\alpha_2\delta$  channels (in the absence of the Ca<sub>v</sub> $\beta$  subunit) and cDNA encod-

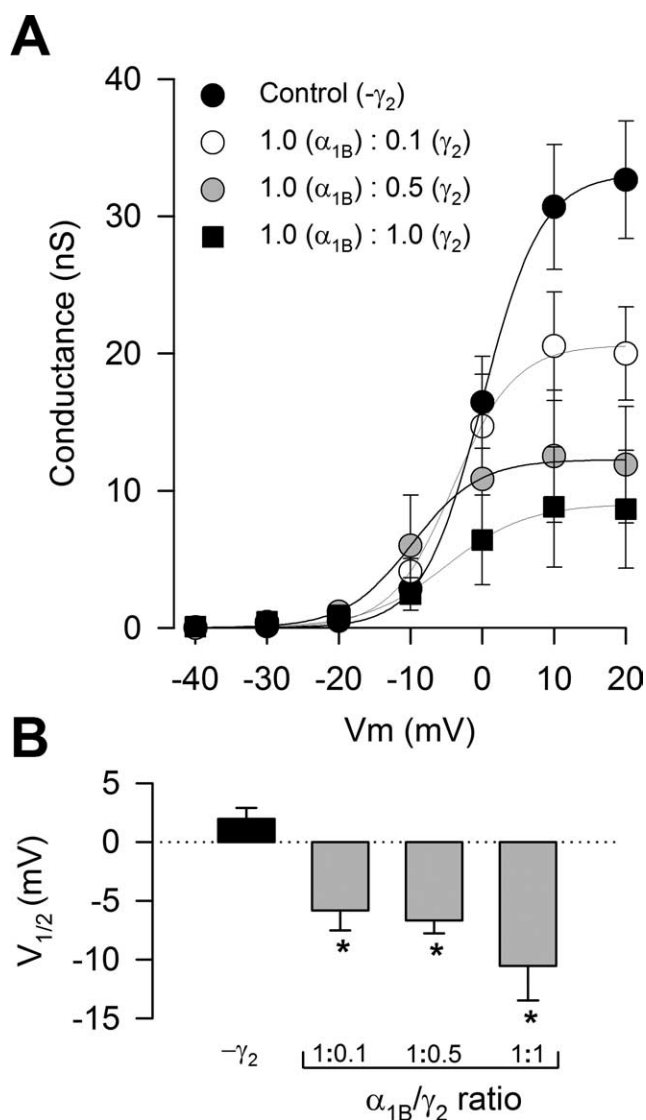


**Figure 3.** The Ca<sub>v</sub> $\gamma_2$  subunit regulates whole-cell conductance. **A**, Voltage dependence of activation of recombinant N-type [Ca<sub>v</sub>2.2( $\alpha_{1B}$ )/Ca<sub>v</sub> $\alpha_2\delta$ /Ca<sub>v</sub> $\beta_3$ ] channels in control cells ( $-\gamma_2$ ) or cells cotransfected with different concentrations of the cDNA encoding the Ca<sub>v</sub> $\gamma_2$  subunit. Conductance data were derived from Figure 2B using the expression:  $G = I/(V_m - V_{rev})$ , where *I* is current, *G* is conductance, *V<sub>m</sub>* is the test potential, and *V<sub>rev</sub>* is the extrapolated reversal potential. The mean data were fitted with Boltzmann functions of the form  $G = G_{max}/(1 + \exp[(V_m - V_{1/2})/k]^{-1})$ , where *G<sub>max</sub>* is maximum conductance, *V<sub>m</sub>* is the test potential, *V<sub>1/2</sub>* is the potential for half-maximal activation of *G<sub>max</sub>*, and *k* is a slope factor. **B**, Comparison of the mean half-activation voltage (*V<sub>1/2</sub>*) for Ca<sub>v</sub>2.2/Ca<sub>v</sub> $\alpha_2\delta$ /Ca<sub>v</sub> $\beta_3$  channels alone ( $-\gamma_2$ ) or coexpressed with the Ca<sub>v</sub> $\gamma_2$  subunit (*n* = 12–14). Error bars indicate SEM, and the asterisks denote significant differences (*p* < 0.05) compared with control.

ing Ca<sub>v</sub> $\gamma_2$  or Ca<sub>v</sub> $\gamma_3$  at a molar ratio of 1:1. As shown by representative current traces (Fig. 5A, top), the presence of Ca<sub>v</sub> $\gamma$  subunits results in a significant reduction of current amplitude. Consequently, the comparison of mean current density at +10 mV recorded in HEK-293 cells expressing Ca<sub>v</sub>2.2/ $\alpha_2\delta$  channels and cells coexpressing the Ca<sub>v</sub> $\gamma$  subunits resulted in current densities of ~60 and ~30%, respectively (Fig. 5A, bottom). We then performed this experiment in cells transfected with different concentrations of the Ca<sub>v</sub> $\alpha_2\delta$  cDNA. As shown in Figure 5B, Ca<sub>v</sub> $\gamma_2$  coexpression led to suppression of Ca<sub>v</sub>2.2 currents even at low Ca<sub>v</sub> $\alpha_2\delta$  cDNA concentrations, although, as expected, the inhibitory effects were less pronounced as the relative molar ratio of Ca<sub>v</sub> $\alpha_2\delta$  increased.

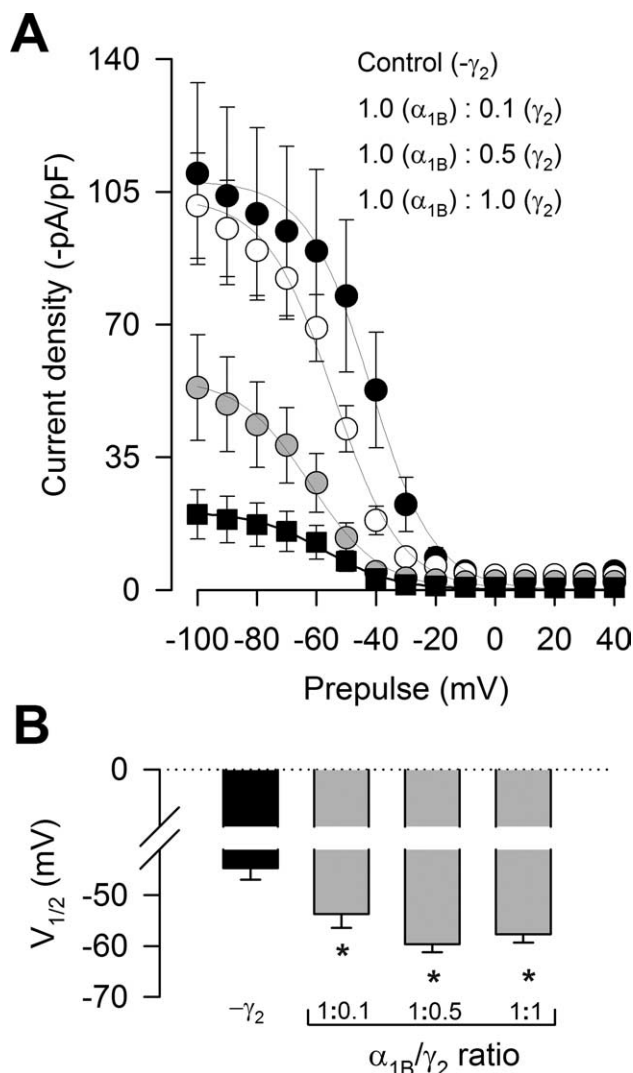


**Figure 4.** Ca<sub>v</sub> $\gamma_2$  regulates Ca<sub>v</sub>2.2( $\alpha_{1B}$ )/Ca<sub>v</sub> $\alpha_2\delta$ /Ca<sub>v</sub> $\beta_3$  channel steady-state inactivation. **A**, Voltage dependence of steady-state inactivation of N-type recombinant channels in the absence and presence of Ca<sub>v</sub> $\gamma_2$ . Currents were recorded after conditioning pulses of 2 s duration, applied from a holding potential of  $-80$  mV in 10 mV steps between  $-100$  and  $+40$  mV, followed by a 140 ms test pulse to  $+10$  mV. Data are plotted against the conditioning potentials ( $n = 6-12$ ). The mean data were fitted with a Boltzmann function of the following form:  $I_{Ba} = I_{max}/(1 + \exp((V_m - V_{1/2})/k))$ , where the current amplitude  $I_{Ba}$  has decreased to a half-amplitude at  $V_{1/2}$  with an  $e$ -fold change over  $k$  mV. **B**, Comparison of the mean half-inactivation voltage ( $V_{1/2}$ ) for Ca<sub>v</sub>2.2/Ca<sub>v</sub> $\alpha_2\delta$ /Ca<sub>v</sub> $\beta_3$  channels alone ( $-\gamma_2$ ) or coexpressed with the Ca<sub>v</sub> $\gamma_2$  subunit ( $n = 6-12$ ). The asterisks denote significant differences ( $p < 0.05$ ) compared with control. Error bars indicate SEM.

Similar suppression effects were observed when the HEK-293 cells expressing Ca<sub>v</sub>2.2/ $\beta$  channels were cotransfected with the cDNA coding for Ca<sub>v</sub> $\gamma_2$  or Ca<sub>v</sub> $\gamma_3$ . Representative superimposed  $I_{Ba}$  traces show Ca<sub>v</sub> $\gamma$ -mediated reduction of N-type current (Fig. 6A, top). Notably, the inhibitory effect of the Ca<sub>v</sub> $\gamma$  subunits is evident even in the absence of the Ca<sub>v</sub> $\alpha_2\delta$  subunit. Comparing the mean current densities at  $+10$  mV, coexpression with Ca<sub>v</sub> $\gamma_2$  or Ca<sub>v</sub> $\gamma_3$  (molar ratios of 1:1) resulted in  $I_{Ba}$  densities of  $\sim 15$  and  $\sim 25\%$ , respectively (Fig. 6A, bottom). Lastly, when this experiment was performed in cells transfected with various concentrations of Ca<sub>v</sub> $\beta$ , coexpression of the Ca<sub>v</sub> $\gamma_2$  subunit decreased  $I_{Ba}$  density at all concentrations tested, and, as in the case of the Ca<sub>v</sub> $\alpha_2\delta$  subunit, increased molar coexpression of Ca<sub>v</sub> $\beta$  did not counteract the inhibitory effects of Ca<sub>v</sub> $\gamma_2$  (Fig. 6B).

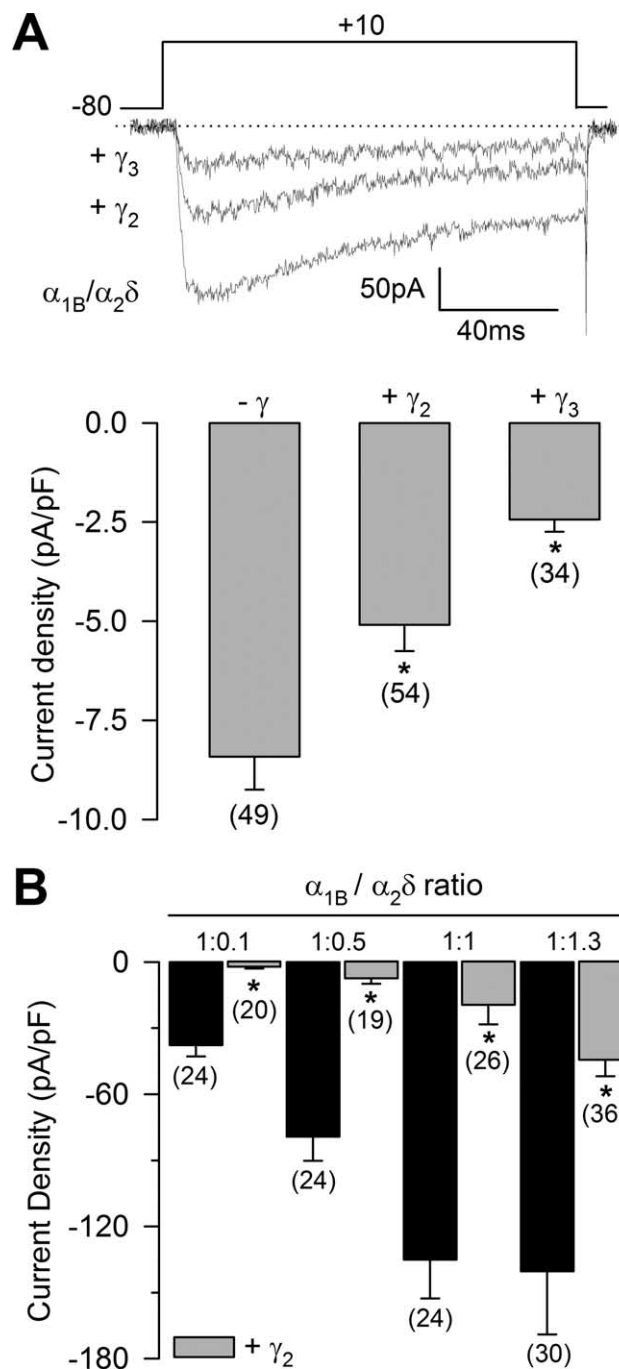


**Figure 5.** Regulation of Ca<sub>v</sub>2.2 channel currents by Ca<sub>v</sub> $\gamma_2$  is not dependent on the presence of the Ca<sub>v</sub> $\beta$  auxiliary subunits. **A**, Representative current traces from control cells [HEK-293 cells expressing Ca<sub>v</sub>2.2( $\alpha_{1B}$ )/ $\alpha_2\delta$  channels in absence of the Ca<sub>v</sub> $\beta$  subunit] and cells coexpressing either the Ca<sub>v</sub> $\gamma_2$  or the Ca<sub>v</sub> $\gamma_3$  subunits. Currents were elicited by voltage steps to  $+10$  mV from a holding potential of  $-80$  mV. Bottom, Comparison of  $I_{Ba}$  density in HEK-293 cells determined as the current amplitude at  $V_m$  of  $+10$  mV normalized by cell capacitance (picoamperes per picofarad). **B**,  $I_{Ba}$  density determined in cells cotransfected with Ca<sub>v</sub>2.2/ $\beta_3$  and varying molar ratios of the cDNA for the Ca<sub>v</sub> $\alpha_2\delta$  subunit in absence (black bars) and presence of Ca<sub>v</sub> $\gamma_2$  (gray bars). The number of recorded cells is listed in parentheses. The asterisks denote significant differences ( $p < 0.05$ ) compared with control.

#### The actions of Ca<sub>v</sub> $\gamma_2$ and Ca<sub>v</sub> $\gamma_3$ are not prevented by inhibition of internalization

The preceding data indicated that heterologous expression of the Ca<sub>v</sub> $\gamma_2$  subunit substantially reduced  $I_{Ba}$  density through recombinant N-type Ca<sup>2+</sup> channels in HEK-293 cells by altering the

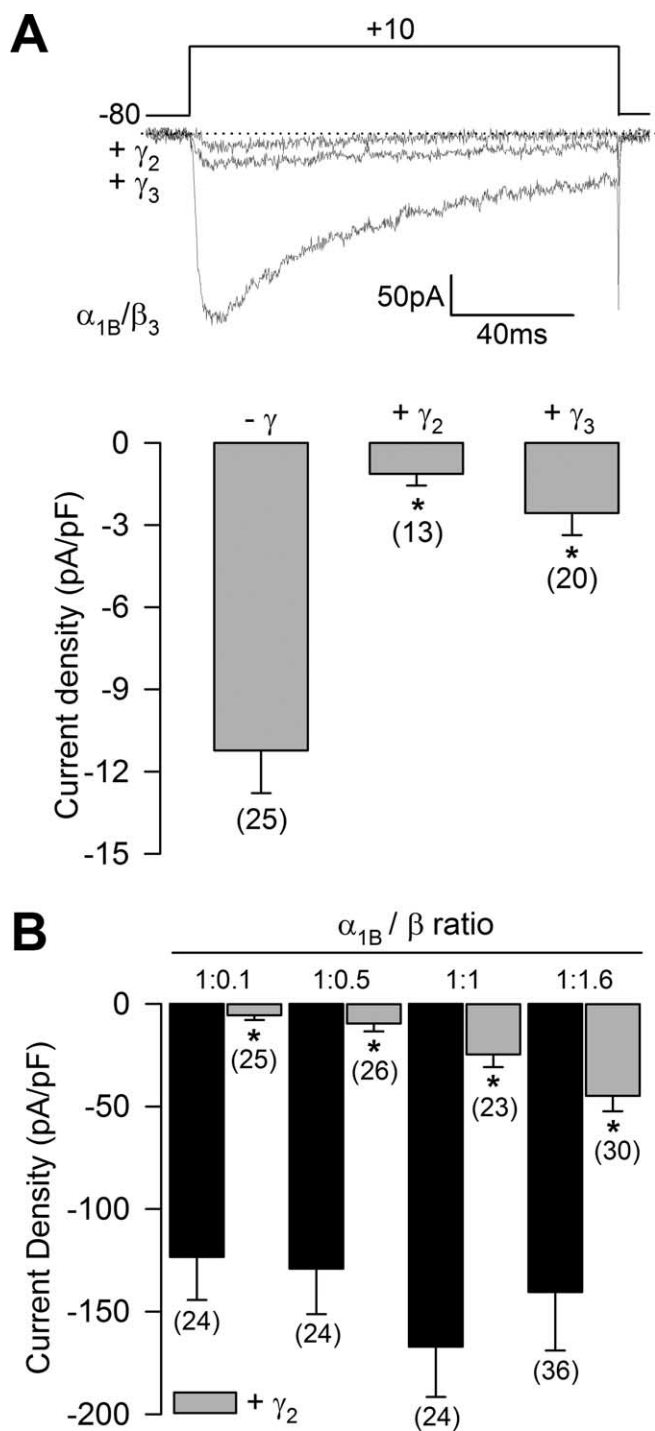


**Figure 6.** Regulation of Ca<sub>v</sub>2.2 channel currents by Ca<sub>v</sub>2.2  $\gamma_2$  is not dependent on the presence of Ca<sub>v</sub> $\alpha_2\delta$ . **A**, Superimposed whole-cell current traces from control cells [HEK-293 cells expressing Ca<sub>v</sub>2.2( $\alpha_{1B}$ )/ $\beta_3$  channels in the absence of the Ca<sub>v</sub> $\alpha_2\delta$  subunit] and cells coexpressing either the Ca<sub>v</sub> $\gamma_2$  or the Ca<sub>v</sub> $\gamma_3$  subunits. Bottom, Comparison of  $I_{Ba}$  density in HEK-293 cells determined at  $V_m$  of +10 mV. **B**,  $I_{Ba}$  density determined in cells cotransfected with Ca<sub>v</sub>2.2/ $\alpha_2\delta$  and varying molar ratios of the cDNA for Ca<sub>v</sub> $\beta_3$  in absence (black bars) and presence of the Ca<sub>v</sub> $\gamma_2$  subunit (gray bars). The number of recorded cells is listed in parentheses. The asterisks denote significant differences ( $p < 0.05$ ) compared with control.

whole-cell conductance and the balance between channel availability and inactivation. However, the shift in the voltage dependence of channel inactivation ( $\sim 15$  mV in the hyperpolarizing direction) only reduces the fraction of available channels by  $\sim 10\%$  at a holding potential of  $-80$  mV, and thus cannot fully

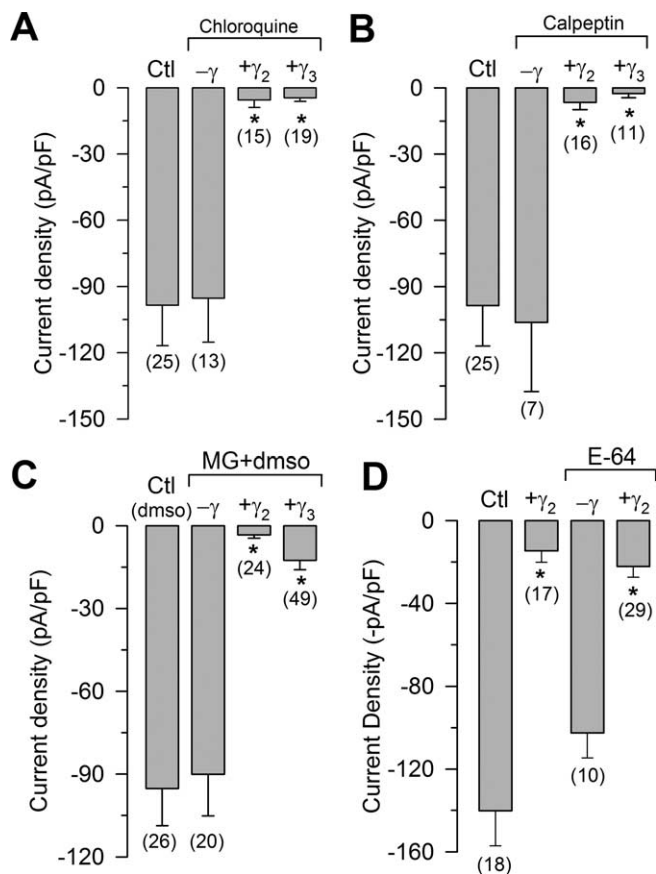


**Figure 7.** The actions of the Ca<sub>v</sub> $\gamma_2$  and Ca<sub>v</sub> $\gamma_3$  subunits are not prevented by inhibition of internalization. **A**, **B**, Mean  $I_{Ba}$  density in HEK-293 cells expressing Ca<sub>v</sub>2.2/Ca<sub>v</sub> $\alpha_2\delta$ /Ca<sub>v</sub> $\beta_3$ /Ca<sub>v</sub> $\gamma_2$  subunits before (control) and after application of chloroquine (100  $\mu\text{M}$ ) and calpeptin (40  $\mu\text{M}$ ) at 37°C for 6 h, respectively. **C**, Mean  $I_{Ba}$  density in transfected HEK-293 cells before and after application of MG-132 (25  $\mu\text{M}$  at 37°C for 6 h). Control cells (expressing Ca<sub>v</sub>2.2/Ca<sub>v</sub> $\alpha_2\delta$ /Ca<sub>v</sub> $\beta_3$  channels in absence of the Ca<sub>v</sub> $\gamma$  subunits) were incubated for 6 h in the presence of the drug (MG-132) or the vehicle alone (dms). **D**, Mean  $I_{Ba}$  density in nonexpressing Ca<sub>v</sub> $\gamma$  HEK-293 cells (control), and cells cotransfected with Ca<sub>v</sub>2.2/Ca<sub>v</sub> $\alpha_2\delta$ /Ca<sub>v</sub> $\beta_3$ /Ca<sub>v</sub> $\gamma_2$  before (+ $\gamma_2$ ) and after (+ $\gamma_2$  E-64) acute exposure to the protease inhibitor E-64 (50  $\mu\text{M}$  at 37°C for 6 h). In all cases, currents were elicited by depolarizing test pulses to +10 mV from a holding potential of  $-80$  mV. Bars denote mean  $\pm$  SE; the number of recorded cells is indicated in parentheses. The asterisks denote significant differences ( $p < 0.05$ ) compared with control.

explain the drastic inhibitory effects observed in  $I_{Ba}$  density in the presence of the inhibitory subunit. This suggested the possibility that the channels could be removed from the cell surface after Ca<sub>v</sub> $\gamma_2$  expression. To analyze the possible participation of a Ca<sub>v</sub> channel internalization-dependent mechanism, a series of inhibitors were used. First, we tested the lysosomal inhibitor chloroquine and the calpain antagonist calpeptin. Chloroquine is a weak base that accumulates in lysosomes, dissipating the acidic pH, whereas calpeptin is a general inhibitor of calpain-induced protein breakdown necessary for the activity of the ubiquitin-proteasome system. Both compounds have been used to inhibit internalization. The data in Figure 7, **A** and **B**, show that N-type  $I_{Ba}$  density was similarly reduced in cells transfected with Ca<sub>v</sub> $\gamma_2$  or Ca<sub>v</sub> $\gamma_3$  even in the presence of the internalization inhibitors, from a control value of  $-98.6 \pm 18.4$  to  $-5.5 \pm 3.5$  and  $-4.7 \pm 1.6$  pA/pF, in the case of chloroquine, and to  $-6.7 \pm 3.2$  and  $-2.5 \pm 1.9$  pA/pF in the case of calpeptin.

To examine in more detail whether the Ca<sub>v</sub> $\gamma$ -mediated current decrease involved internalization of the channels, we evaluated the effects of MG-132 and E-64. MG-132, a selective inhib-

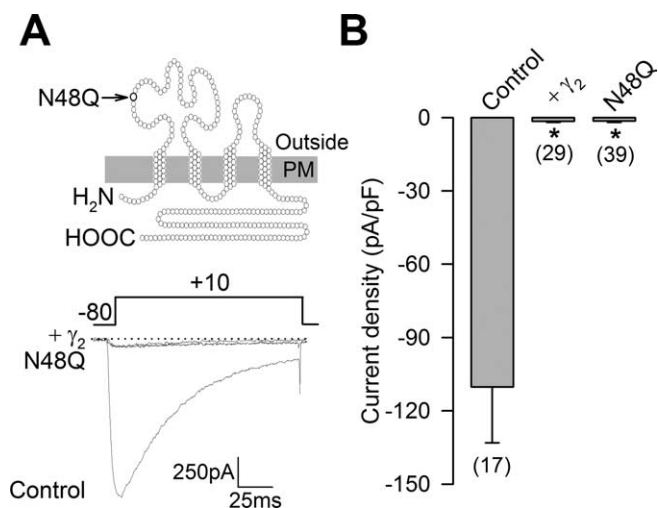


**Figure 8.** Mutation at site N48 in the first extracellular loop does not disrupt the function of Ca<sub>v</sub> $\gamma_2$ . **A**, Schematic representation of the Ca<sub>v</sub> $\gamma_2$  subunit. The position of the asparagine residue substituted is indicated. Bottom, Superimposed representative whole-cell Ba<sup>2+</sup> current traces through Ca<sub>v</sub>2.2/Ca<sub>v</sub> $\alpha_2\delta$ /Ca<sub>v</sub> $\beta_3$  in HEK-293 cells in the absence of the Ca<sub>v</sub> $\gamma$  subunit (control) and cells expressing the wild-type Ca<sub>v</sub> $\gamma_2$  (+ $\gamma_2$ ) or the N → Q mutant (N48Q). Currents were generated by applying 140 ms activating pulses at +10 mV from a holding potential of -80 mV. **B**, Mean  $I_{Ba}$  density in HEK-293 cells as in **A**. Bars denote mean  $\pm$  SE; the number of recorded cells is indicated in parentheses. \* $p$  < 0.05 compared with control.

itor of the 26S proteasome, failed to alter the inhibitory actions of Ca<sub>v</sub> $\gamma_2$  and Ca<sub>v</sub> $\gamma_3$  subunits as  $I_{Ba}$  reduction persisted after drug treatment (Fig. 7C). Similar results were obtained with E-64, a cysteine protease inhibitor that interferes with internalization. Ca<sub>v</sub> $\gamma_2$  decreased  $I_{Ba}$  density through Ca<sub>v</sub>2.2/ $\beta_3$ / $\alpha_2\delta$  channels by 9.6-fold. This effect could not be prevented by the treatment with E-64 (Fig. 7D). Together, these data indicate that the Ca<sub>v</sub> $\gamma$ -mediated reduction of N-type current does not involve a mechanism of enhancing channel internalization.

#### N-linked protein glycosylation is not a major determinant for Ca<sub>v</sub> $\gamma_2$ regulation of recombinant Ca<sub>v</sub>2.2 channels

Previous studies have shown that at least one consensus site for N-linked glycosylation is present in all eight Ca<sub>v</sub> $\gamma$  subunits (Arikkath and Campbell, 2003; Kang and Campbell, 2003), suggesting that such posttranslational modification may have important functions in the Ca<sub>v</sub> channel complex. Interestingly, mutation of this site alters the role of Ca<sub>v</sub> $\gamma_2$  in cell aggregation presumably by preventing the protein from localizing to the plasma membrane (Price et al., 2005). To define the role of this consensus N-glycosylation site in plasma membrane targeting and downregulation of Ca<sub>v</sub> channels, we generated a mutant subunit by substituting glutamine for asparagine at amino acid position 48 of Ca<sub>v</sub> $\gamma_2$  (N48Q) (Fig. 8A, top). In the absence of Ca<sub>v</sub> $\gamma_2$ , control current levels ranged up to 1.3 nA, with an average peak current density of -110  $\pm$  23 pA/pF. Unexpectedly, coexpression of the Ca<sub>v</sub> $\gamma_2$ N48Q variant led to near complete inhibition of  $I_{Ba}$ , similar to that of the wild-type Ca<sub>v</sub> $\gamma_2$  subunit (-1.5  $\pm$  0.4 and -1.4  $\pm$  0.5 pA/pF, respectively) (Fig. 8B). These data suggest that N-type current downregulation may not require efficient Ca<sub>v</sub> $\gamma_2$  trafficking to the cell membrane.

#### Ca<sub>v</sub> $\gamma_2$ -mediated decrease in $I_{Ba}$ density may involve altered Ca<sub>v</sub> channel synthesis and activation of the UPR

Ca<sub>v</sub> $\gamma_2$  effects on N-type channel properties (see above) demonstrate that Ca<sub>v</sub> $\gamma_2$  influences channels at the cell surface. However,

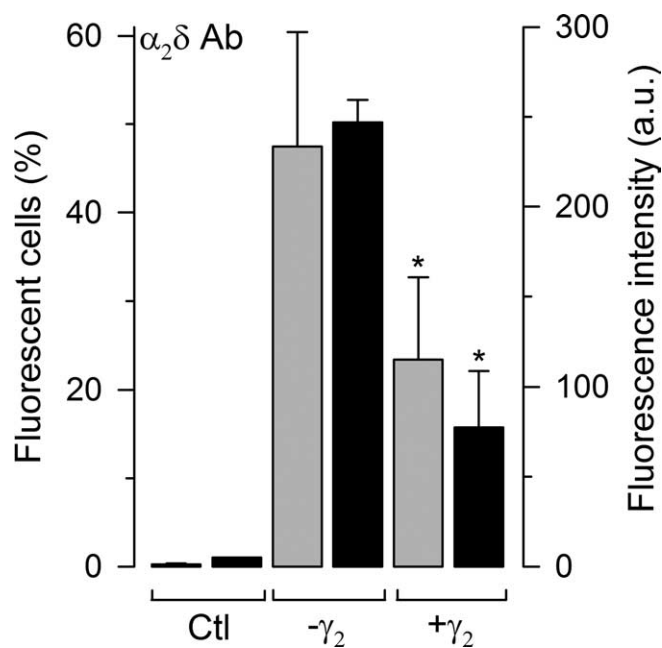


**Figure 9.** Reduction of macroscopic N-type current after Ca<sub>v</sub> $\gamma_2$  transfection may involve alterations in surface expression and interference with the synthesis of new channels. Flow cytometric analysis of the percentage of fluorescent cells and fluorescence intensity in untransfected HEK-293 cells, cells expressing Ca<sub>v</sub>2.2/Ca<sub>v</sub> $\alpha_2\delta$ /Ca<sub>v</sub> $\beta_3$  channels (control), and cells co-transfected with the recombinant N-type channels plus the Ca<sub>v</sub> $\gamma_2$  subunit (+ $\gamma_2$ ). The histograms denote mean  $\pm$  SEM values, and the data are representative of two independent experiments of channels probed with an anti-Ca<sub>v</sub> $\alpha_2\delta$  affinity-purified antibody. Samples were run in triplicate and 1–2  $\times$  10<sup>4</sup> cells were measured per run. The asterisks denote significant differences ( $p$  < 0.05) compared with control. Ab, Antibody; Ctl, control untransfected cells.

our data indicated that  $I_{Ba}$  reduction after Ca<sub>v</sub> $\gamma_2$  transfection may also involve alterations in surface expression or interference with the synthesis of new channels. Because we ruled out the possibility that Ca<sub>v</sub> $\gamma_2$  could increase channel internalization, we next investigated a potential inhibition of channel synthesis. To examine this, an EGFP-Ca<sub>v</sub>2.2 fusion construct was heterologously expressed in the HEK-293 cells together with the Ca<sub>v</sub> $\beta$  and Ca<sub>v</sub> $\alpha_2\delta$  subunits, and the fluorescence emissions in presence and absence of Ca<sub>v</sub> $\gamma_2$  were quantified using flow cytometry. Coexpression of Ca<sub>v</sub> $\gamma_2$  with the tagged N-type channel reduced the percentage of GFP-expressing cells to  $\sim$ 39  $\pm$  2 from  $\sim$ 48  $\pm$  3% obtained in the absence of Ca<sub>v</sub> $\gamma_2$  (data not shown). Interestingly, coexpression of Ca<sub>v</sub> $\gamma_2$  also reduced the average fluorescence intensity per fluorescence-positive HEK-293 cells to  $\sim$ 285  $\pm$  9 from 354  $\pm$  8 arbitrary units in the control cells.

It should be noted that, under these conditions, flow cytometry is not well suited to distinguish fluorescence originating from the plasma membrane versus the cytoplasm. To investigate whether the number of the channels expressed at the cell surface was also altered, we performed flow cytometry experiments using an affinity-purified primary antibody against an extracellular epitope in the Ca<sub>v</sub> $\alpha_2\delta$  subunit. As summarized in Figure 9, both the percentage of Ca<sub>v</sub> $\alpha_2\delta$ -immunopositive cells and the mean fluorescence intensity significantly decreased when Ca<sub>v</sub> $\gamma_2$  was coexpressed. The proportion of immunoreactive cells was reduced to  $\sim$ 23  $\pm$  9% in the Ca<sub>v</sub> $\gamma_2$ -expressing cells from  $\sim$ 47  $\pm$  13% observed in the controls. Likewise, coexpression of the Ca<sub>v</sub> $\gamma_2$  subunit decreased the average fluorescence intensity  $\sim$ 70% compared with control cells (+Ca<sub>v</sub> $\gamma_2$ ,  $\sim$ 77  $\pm$  31; -Ca<sub>v</sub> $\gamma_2$ ,  $\sim$ 247  $\pm$  13 arbitrary units), which may help to explain the reduction in N-type current density on Ca<sub>v</sub> $\gamma_2$  expression.

Together, these results strongly suggested that the decrease in  $I_{Ba}$  density caused by Ca<sub>v</sub> $\gamma_2$  expression involved an inhibition of Ca<sub>v</sub> channel synthesis without compensatory alterations in channel internalization. In this regard, it is worth mentioning that the expression of truncated versions of Ca<sub>v</sub>2.2 causes channel synthesis arrest at an early stage (Raghib et al., 2001). Likewise, it has been reported that the expression of a short variant of Ca<sub>v</sub>2.1 markedly suppresses currents presumably through the activation of an endoplasmic reticulum-resident RNA-dependent kinase (PERK), which activates components of the UPR to suppress Ca<sub>v</sub>2.1 translation (Page et al., 2004).

Notably, our results with the Ca<sub>v</sub> $\gamma_2$  subunit bear a striking resemblance to the dominant-negative synthesis suppression of the Ca<sub>v</sub>2 subunits induced by the coexpression of truncated constructs. Therefore, we tested whether Ca<sub>v</sub>2.2 current suppression by Ca<sub>v</sub> $\gamma_2$  involved activation of the UPR. Initially, we investigated the effects of genistein, a tyrosine kinase inhibitor that prevents full expression of the UPR through inactivation of the transcription factor NF-Y (nuclear factor Y) (Zhou and Lee, 1998; Nyfeler et al., 2003). After 6 h treatment with the drug (140  $\mu$ M), there was no significant change in  $I_{Ba}$  density of Ca<sub>v</sub> $\gamma_2$ -expressing cells (Fig. 10). In contrast, longer exposure (24 h) to genistein resulted in a significant reduction of the suppressive effect of Ca<sub>v</sub> $\gamma_2$ . These findings suggested that activation of the UPR might play a role in the suppression of Ca<sub>v</sub>2.2 currents by the Ca<sub>v</sub> $\gamma_2$  auxiliary subunit.

To confirm that Ca<sub>v</sub> $\gamma_2$  expression promotes N-type channel regulation via the unfolded protein response mechanism, we used a strategy analogous to that reported by Dolphin and colleagues (Page et al., 2004). This approach consisted in the expression of two dominant-negative PERK constructs. The first construct encodes a PERK lacking the C-terminal kinase domain (PERK  $\Delta$ C), whereas the second construct encodes a PERK with a point mutation in the catalytic site (PERK K618A). Both constructs have been shown to prevent the activation of endogenous PERK (Harding et al., 1999) and therefore inhibit the UPR. When dominant-negative PERK constructs were expressed with the Ca<sub>v</sub> $\gamma_2$  subunit and N-type (Ca<sub>v</sub>2.2/ $\beta_3/\alpha_2\delta$ ) channels, there was a significant reversal of Ca<sub>v</sub> $\gamma_2$ -mediated current suppression (Fig. 11). With the PERK  $\Delta$ C mutation, Ca<sub>v</sub> $\gamma_2$ -mediated  $I_{Ba}$  inhibition was significantly diminished from  $\sim$ 94 to  $\sim$ 74%, whereas PERK K618A also reduced the suppressive effect of Ca<sub>v</sub> $\gamma_2$  to  $\sim$ 66% (Fig. 11B). These results indicate that activation of PERK may play an important role in the suppression of Ca<sub>v</sub>2.2 currents by the Ca<sub>v</sub> $\gamma_2$  regulatory subunit.

### Ca<sub>v</sub> $\gamma_2$ inhibits Ca<sup>2+</sup> channel activity in DRG neurons

We lastly sought to determine whether the inhibitory actions of Ca<sub>v</sub> $\gamma_2$  were also present on native neuronal Ca<sub>v</sub> channels. To this end, we analyzed the  $I_{Ba}$  density in neonatal mouse DRG neurons transiently transfected with GFP or with the pAd5CMVK-NpA construct (containing the Ca<sub>v</sub> $\gamma_2$  subunit plus the GFP).  $I_{Ba}$  through native Ca<sup>2+</sup> channels were analyzed by the whole-cell mode of the patch-clamp technique (Fig. 12). Only cells with a robust GFP fluorescence signal were used for electrophysiological recording. DRG neurons transfected with GFP construct produced current amplitudes of  $\sim$ 1 nA. Interestingly, the exogenous expression of the Ca<sub>v</sub> $\gamma_2$  produced significantly smaller current amplitudes (Fig. 12B). Likewise, the expression of the auxiliary subunit in DRG neurons did not significantly change the capacitance of the cells (data not shown). As a result, in comparison with the control condition, the expression of Ca<sub>v</sub> $\gamma_2$  causes a sub-

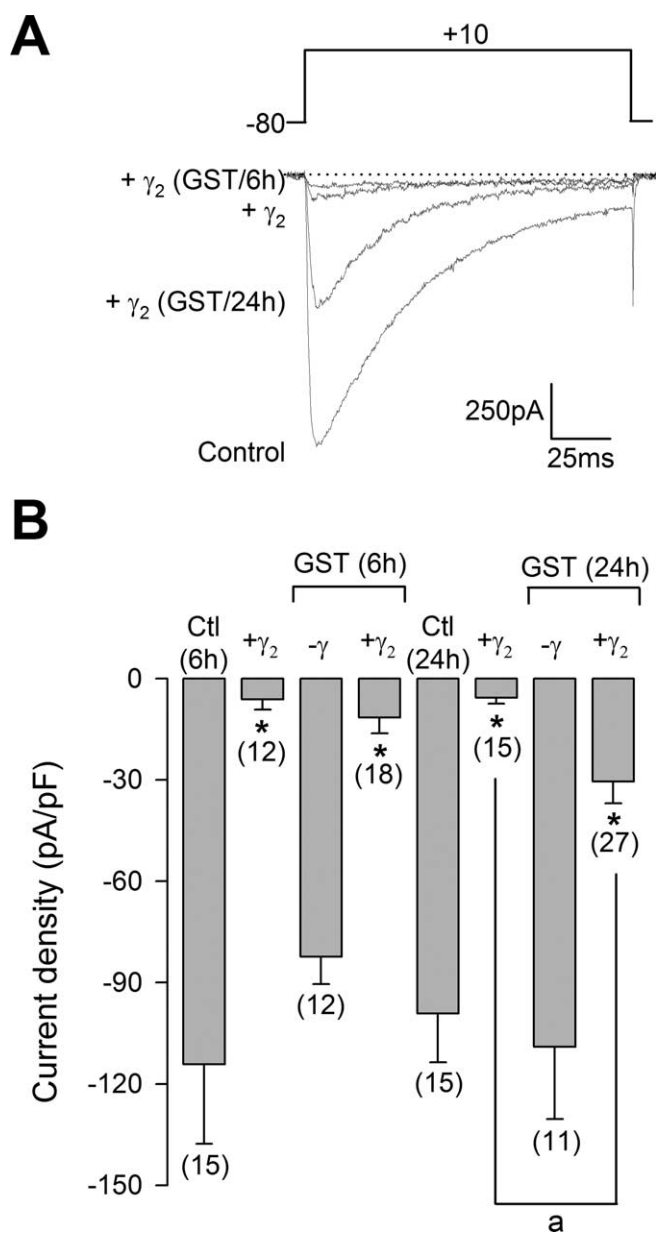


**Figure 10.** Extracellular application of genistein, an inhibitor of the UPR, antagonizes the suppressive effect of Ca<sub>v</sub> $\gamma_2$  on the N-type current expressed in the HEK-293 cells. **A**, Representative Ba<sup>2+</sup> currents through recombinant N-type channels obtained in HEK-293 cells expressing Ca<sub>v</sub>2.2/Ca<sub>v</sub> $\alpha_2\delta$ /Ca<sub>v</sub> $\beta_3$  channels either in the absence (control) or presence of Ca<sub>v</sub> $\gamma_2$  plus genistein (140  $\mu$ M at 37°C for 6 or 24 h). Control conditions included exposure to  $\sim$ 0.1% dimethyl sulfoxide (the vehicle for genistein). Currents were evoked by step depolarizations to +10 mV from a holding potential of  $-80$  mV. **B**, Mean  $I_{Ba}$  density in transfected HEK-293 cells as in **A**. Statistical significance ( $p < 0.05$ ) compared with respective control (\*) or Ca<sub>v</sub> $\gamma_2$  plus vehicle alone (a) is indicated. Ctl, Control; GST, genistein.

stantial decrease in current density through Ca<sub>v</sub> channels in mouse neonatal DRG neurons.

### Discussion

In the current report, we show that the neuronal Ca<sub>v</sub> $\gamma_2$  and Ca<sub>v</sub> $\gamma_3$  subunits exert an important inhibitory effect on currents through recombinant N-type Ca<sup>2+</sup> channels heterologously expressed in HEK-293 cells. This inhibition is (1) specific to Ca<sub>v</sub> channels given that Ca<sub>v</sub> $\gamma$  subunit coexpression did not affect endogenous K<sup>+</sup> current, (2) restricted to HVA channels because currents through recombinant LVA channels were not affected,

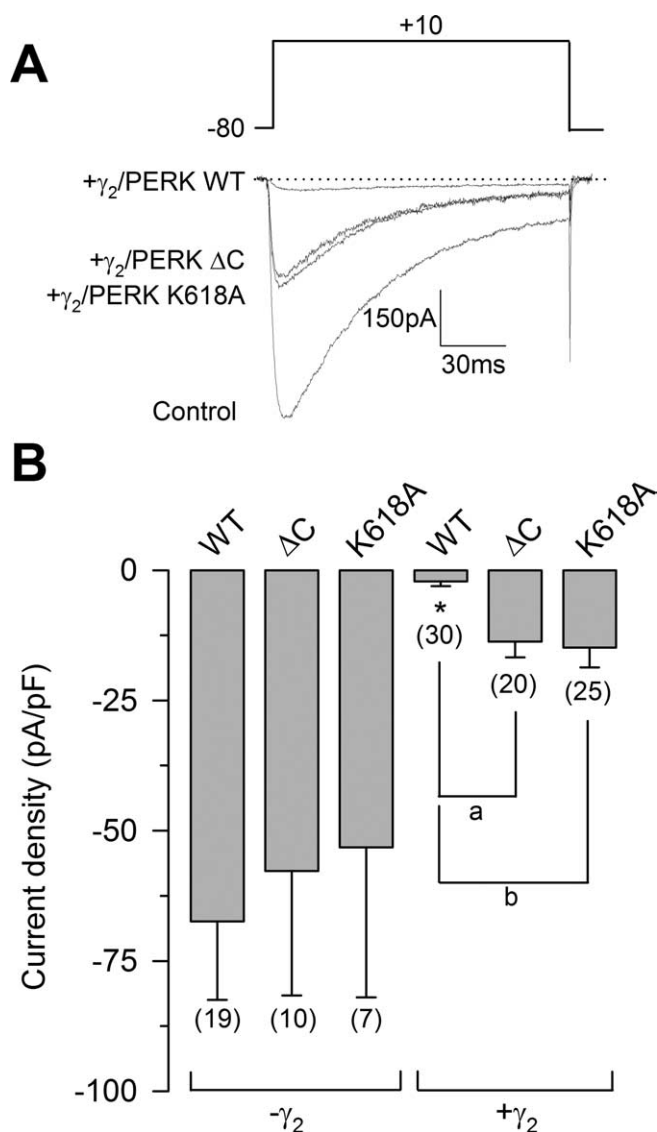


**Figure 11.** Coexpression of two dominant-negative constructs of the endoplasmic reticulum-resident RNA-dependent kinase (PERK) causes a reversal of current suppression observed after transfection of Ca<sub>v</sub> $\gamma_2$ . **A**, Examples of Ba<sup>2+</sup> currents elicited by 140 ms depolarizing pulses to +10 mV from a holding potential of -80 mV in HEK-293 cells expressing Ca<sub>v</sub>2.2/Ca<sub>v</sub> $\alpha_2\delta$ /Ca<sub>v</sub> $\beta_3$  channels either in the absence (control) or presence of Ca<sub>v</sub> $\gamma_2$  plus wild-type PERK, or the mutant constructs PERK  $\Delta$ C and PERK K618A. **B**, Mean  $I_{Ba}$  density in transfected HEK-293 cells as in **A**. Statistical significance ( $p < 0.05$ ) compared with control (\*) or wild-type PERK (a, b) is indicated.

(3) not mimicked by an unrelated tetraspan protein, and (4) observed in the absence of the other Ca<sub>v</sub> regulatory subunits. These findings are consistent with previous reports that Ca<sub>v</sub> $\gamma$  subunit coexpression generally reduces current density through recombinant channels (Kang et al., 2001; Moss et al., 2002; Arikath et al., 2003; Hansen et al., 2004).

An interesting issue to be clarified relates to cell pathways by which this Ca<sub>v</sub> $\gamma$ -mediated inhibition occurs. As we discuss in the following sections, distinct mechanisms could underlie the decrease in  $I_{Ba}$  density after Ca<sub>v</sub> $\gamma$  expression.

#### Alteration in the functioning of the channels

In addition to decreasing peak current density, patch-clamp recordings showed that Ca<sub>v</sub> $\gamma$  subunits alter the voltage dependency of activation and inactivation of recombinant Ca<sub>v</sub>2.2/ $\beta_3$ / $\alpha_2\delta$

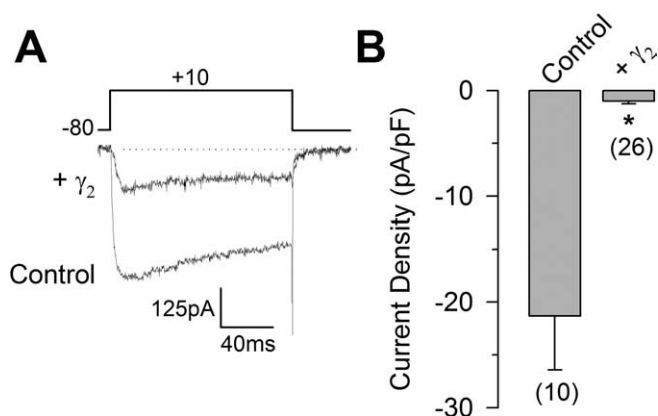


**Figure 12.** Ca<sub>v</sub> $\gamma_2$  transfection inhibits Ca<sup>2+</sup> channel activity in neonatal DRG neurons. **A**, Representative traces of whole-cell  $I_{Ba}$  through Ca<sub>v</sub> channels in cultured DRG neurons transfected with either GFP alone (control) and GFP plus Ca<sub>v</sub> $\gamma_2$ . The currents were evoked by a single depolarizing step from a holding potential of -80 to +10 mV for 140 ms. **B**, Comparison of averaged peak current density in DRG cells expressing GFP alone (control) and the exogenous Ca<sub>v</sub> $\gamma_2$  subunit. Currents were elicited as in **A**.

channels. Interestingly, a specific effect of Ca<sub>v</sub> $\gamma_2$  on current inactivation has previously been shown for Ca<sub>v</sub>2.1 (Letts et al., 1998; Klugbauer et al., 2000) and Ca<sub>v</sub>1.2 (Klugbauer et al., 2000), suggesting that this property may not be restricted to a particular Ca<sub>v</sub> $\alpha_1$  ion-conducting subunit.

#### Increased channel internalization

Given that regulation of preexisting channels was not sufficient to fully explain Ca<sub>v</sub> $\gamma$ -mediated suppression of N-type currents, a key mechanistic question was whether the channels were removed from the cell surface after coexpression of the auxiliary subunit. According to this, accelerated channel degradation/internalization would lead to a decrease in current density. However, our data seem to firmly rule out this possibility given that the inhibitory actions of the Ca<sub>v</sub> $\gamma_2/\gamma_3$  subunits remained unaltered after treatment of the cells with a series of inhibitors of degradation/internalization (chloroquine, calpeptin, MG-132, and E-64).

#### Inhibition of channel targeting to the cell membrane

Because Ca<sub>v</sub> $\gamma$ -mediated suppression of N-type currents seemed not to involve increased protein internalization, we investigated whether Ca<sub>v</sub> $\gamma_2$  might interfere with the trafficking of Ca<sub>v</sub>2.2 subunits to the cell surface. It is well known that N-linked glycosylation is crucial for the correct folding, subcellular targeting, and stability of numerous proteins (Kleene and Schachner, 2004), including Ca<sub>v</sub> channels (Gurnett et al., 1996; Sandoval et al., 2004). Recently, it has been shown that a mutation in a consensus site for N-glycosylation in the Ca<sub>v</sub> $\gamma_2$  sequence disrupts the ability of the protein to act as a claudin mediating cell–cell adhesion (Price et al., 2005). Consequently, we used the same construct (N48Q) to investigate whether this putative N-glycosylation site mutation could abolish the capability of Ca<sub>v</sub> $\gamma_2$  to act as a regulatory subunit of Ca<sub>v</sub> channels. We reasoned that, if Ca<sub>v</sub> $\gamma_2$  produced a reduction in  $I_{Ba}$  by reducing channel targeting to the plasma membrane, then transfection of the N48Q mutant should prevent suppression of N-type channel activity. However, our results showed that the suppressive effects of the Ca<sub>v</sub> $\gamma_2$  remained unaltered, suggesting that the mutation may alter some of the functional properties of Ca<sub>v</sub> $\gamma_2$ , but may not be important to determine inhibition of N-type channel functional expression.

This is consistent with previous studies showing that treatment with the antibiotic tunicamycin inhibits N-linked glycosylation of the skeletal muscle Ca<sub>v</sub> $\gamma$ <sub>1</sub> subunit but cannot inhibit the association of the auxiliary subunit to the Ca<sub>v</sub>1.1 subunit (Arikkath et al., 2003).

Thus, Ca<sub>v</sub> $\gamma$ <sub>2</sub> may alter Ca<sup>2+</sup> channel function via two distinct pathways. The first pathway, discussed previously, involves modulation of preexisting channels and is suitable for dynamically regulating Ca<sup>2+</sup> channel activity on a rapid timescale. The second pathway, discussed below, may involve interference with Ca<sub>v</sub>2.2 subunit proper folding and synthesis, and would require protein turnover before functional effects are apparent, a mechanism well suited for setting the steady-state level of channels.

### Suppression of channel protein synthesis and prevention of the correct folding of Ca<sub>v</sub>2.2

Seminal work by Dolphin and colleagues indicated that coexpression of the Ca<sub>v</sub> $\gamma$ <sub>7</sub> subunit specifically abolished *I*<sub>Ba</sub> through heterologously expressed Ca<sub>v</sub>2.2 channels and significantly reduced Ba<sup>2+</sup> conductance in non-N type (Ca<sub>v</sub>2.1 and Ca<sub>v</sub>1.2) channels, although the mechanism by which the auxiliary subunit was acting was not determined (Moss et al., 2002). Previous work by these authors also had shown that truncated constructs of the Ca<sub>v</sub>2.2 subunit suppressed Ca<sub>v</sub>2.2 currents and reduced full-length Ca<sub>v</sub>2.2 protein levels by a mechanism that involved decreased synthesis (Raghib et al., 2001). More recently, they found that current suppression required an interaction between the truncated construct and the full-length channel which activates PERK, a component of the UPR, to suppress translation (Page et al., 2004). Remarkably, Ca<sub>v</sub> $\gamma$ <sub>2</sub>-mediated suppression of N-type currents expressed in HEK-293 cells shows resemblance to the inhibition of the Ca<sub>v</sub>2.2 currents induced by the coexpression of truncated Ca<sub>v</sub>2.2 constructs.

When mammalian cells are subjected to ER stress, a specific signaling pathway termed the UPR is triggered. When UPR is initiated, an immediate consequence is the activation of PERK to inhibit protein biosynthesis through phosphorylation of the eukaryotic translation initiation factor eIF2 $\alpha$  (Harding et al., 2002; Marciniak and Ron, 2006). In our study, genistein partially prevented the Ca<sub>v</sub> $\gamma$ <sub>2</sub>-mediated suppression of Ca<sub>v</sub>2.2 currents, suggesting the participation of the UPR. Likewise, we found that the use of protease inhibitors as well as blockers of the proteasome activity did not increase the amount of Ca<sub>v</sub>2.2 currents observed in the presence of Ca<sub>v</sub> $\gamma$ <sub>2</sub>, suggesting that the mechanism does not involve enhanced proteolysis. From these results, the most likely explanation for current suppression by Ca<sub>v</sub> $\gamma$ <sub>2</sub> is that synthesis of the Ca<sub>v</sub>2.2 subunit was arrested. In support of this, flow cytometry analysis indicated that the inhibition of Ca<sub>v</sub>2.2 currents by Ca<sub>v</sub> $\gamma$ <sub>2</sub> may be attributable to a reduction in the number of channels, because there was a significantly reduction in the percentage of fluorescent cells and mean fluorescence intensity of cells coexpressing EGFP-Ca<sub>v</sub>2.2 and the auxiliary subunit.

To examine whether the mechanism of suppression of Ca<sub>v</sub>2.2 expression by Ca<sub>v</sub> $\gamma$ <sub>2</sub> indeed involved the UPR, we used two mutant PERK constructs, PERK  $\Delta$ C and PERK K618A, both of which lack kinase activity. Their dominant-negative behavior arises from their capability to form nonfunctional dimers with endogenous PERK (Harding et al., 1999). Notably, the mutant PERK constructs prevented the inhibition of Ca<sub>v</sub>2.2 expression by the Ca<sub>v</sub> $\gamma$ <sub>2</sub> subunit, implicating activation of the endogenous kinase, and therefore the UPR, in the process of current suppression.

Likewise, it is interesting to consider what physiological role

the Ca<sub>v</sub> $\gamma$ <sub>2</sub>/ $\gamma$ <sub>3</sub> subunit-induced suppression of N-type Ca<sub>v</sub> channels may play. It is well known that this type of channels is expressed predominantly in presynaptic nerve terminals and play a key role in neurotransmitter release (Fisher and Bourque, 2001; Hille, 2001). Given that the Ca<sub>v</sub> $\gamma$ <sub>2</sub>/ $\gamma$ <sub>3</sub> subunits significantly decrease N-type channel activity and expression, they might provide a negative feedback on current amplitude and neurotransmission. In addition, it has been reported that N-type channel expression is an important cue in the genesis of synaptic transmission (Jones et al., 1997; Vance et al., 1998). Therefore, it is also possible that Ca<sub>v</sub> $\gamma$ <sub>2</sub>/ $\gamma$ <sub>3</sub> might play a role as a negative regulator for N-type channel expression during brain ontogeny. Likewise, the expression levels and cell distribution of Ca<sub>v</sub> channel auxiliary subunits can change in diseases such as diabetes (Iwashima et al., 2001), temporal lobe epilepsy (Lie et al., 1999), and neuropathic pain (Luo et al., 2001). Analogously, the Ca<sub>v</sub> $\gamma$  subunits could also play important roles in the pathophysiology of certain channelopathies. In line with this, it has been shown that the removal of the Ca<sub>v</sub> $\gamma$ <sub>2</sub> protein from the brain causes numerous disorders, including spontaneous absence seizures and ataxia in the stargazer mouse mutant (Letts, 2005).

Lastly, considering the role of Ca<sub>v</sub> $\gamma$ <sub>2</sub> as a chaperone protein for proper folding and surface expression of AMPA receptors (Qiao and Meng, 2003), our results suggest some clues concerning a possible multifaceted role for this protein in an individual cell. For instance, in a physiological context in which Ca<sub>v</sub> $\gamma$ <sub>2</sub> expression was low, Ca<sup>2+</sup> influx through Ca<sub>v</sub>2.2 channels would provide a favorable local environment for the stabilization of AMPA receptors at the postsynapsis. However, when Ca<sub>v</sub> $\gamma$ <sub>2</sub> expression was high, Ca<sub>v</sub>2.2 channel synthesis would be negatively modulated, which may result in decreased Ca<sup>2+</sup> influx and a favorable local environment for the lateral movement of AMPA receptors. It is worth mentioning that it has been suggested that indeed changes in local intracellular Ca<sup>2+</sup> may regulate the lateral movement of AMPA receptors in hippocampal neurons (Borgdorff and Choquet, 2002). In this way, the expression of the Ca<sub>v</sub> $\gamma$ <sub>2</sub> subunit could play a role in the molecular mechanism underlying synaptic plasticity.

### References

- Arikkath J, Campbell KP (2003) Auxiliary subunits: essential components of the voltage-gated calcium channel complex. *Curr Opin Neurobiol* 13:298–307.
- Arikkath J, Chen CC, Ahern C, Allamand V, Flanagan JD, Coronado R, Gregg RG, Campbell KP (2003)  $\gamma$ <sub>1</sub> subunit interactions within the skeletal muscle L-type voltage-gated calcium channels. *J Biol Chem* 278:1212–1219.
- Avila G, Sandoval A, Felix R (2004) Intramembrane charge movement associated with endogenous K<sup>+</sup> channel activity in HEK-293 cells. *Cell Mol Neurobiol* 24:317–330.
- Avila T, Andrade A, Felix R (2006) Transforming growth factor-beta1 and bone morphogenetic protein-2 downregulate Ca<sub>v</sub>3.1 channel expression in mouse C2C12 myoblasts. *J Cell Physiol* 209:448–456.
- Berridge MJ (1998) Neuronal calcium signaling. *Neuron* 21:13–26.
- Black III JL (2003) The voltage-gated calcium channel  $\gamma$  subunits: a review of the literature. *J Bioenerg Biomembr* 35:649–660.
- Borgdorff AJ, Choquet D (2002) Regulation of AMPA receptor lateral movements. *Nature* 417:649–653.
- Castellano A, Wei X, Birnbaumer L, Perez-Reyes E (1993) Cloning and expression of a third calcium channel beta subunit. *J Biol Chem* 268:3450–3455.
- Catterall WA, Perez-Reyes E, Snutch TP, Striessnig J (2005) International Union of Pharmacology. XLVIII. Nomenclature and structure-function relationships of voltage-gated calcium channels. *Pharmacol Rev* 57:411–425.
- Cribbs LL, Lee JH, Yang J, Satin J, Zhang Y, Daud A, Barclay J, Williamson

- MP, Fox M, Rees M, Perez-Reyes E (1998) Cloning and characterization of  $\alpha_{1H}$  from human heart, a member of the T-type Ca<sup>2+</sup> channel gene family. *Circ Res* 83:103–109.
- Crosbie RH, Heighway J, Venzke DP, Lee JC, Campbell KP (1997) Sarcospan, the 25-kDa transmembrane component of the dystrophin-glycoprotein complex. *J Biol Chem* 272:31221–31224.
- Felix R (2005) Molecular regulation of voltage-gated Ca<sup>2+</sup> channels. *J Recept Signal Transduct Res* 25:57–71.
- Fisher TE, Bourque CW (2001) The function of Ca<sup>2+</sup> channel subtypes in exocytotic secretion: new perspectives from synaptic and non-synaptic release. *Prog Biophys Mol Biol* 77:269–303.
- Fujita Y, Mynlieff M, Dirksen RT, Kim MS, Niidome T, Nakai J, Friedrich T, Iwabe N, Miyata T, Furuichi T, Furutama D, Mikoshiba K, Mori Y, Beam KG (1993) Primary structure and functional expression of the  $\omega$ -conotoxin-sensitive N-type calcium channel from rabbit brain. *Neuron* 10:585–598.
- Gurnett CA, De Waard M, Campbell KP (1996) Dual function of the voltage-dependent Ca<sup>2+</sup> channel  $\alpha_2\delta$  subunit in current stimulation and subunit interaction. *Neuron* 16:431–440.
- Hansen JP, Chen RS, Larsen JK, Chu PJ, Janes DM, Weis KE, Best PM (2004) Calcium channel  $\gamma_6$  subunits are unique modulators of low voltage-activated (Cav3.1) calcium current. *J Mol Cell Cardiol* 37:1147–1158.
- Harding HP, Zhang Y, Ron D (1999) Protein translation and folding are coupled by an endoplasmic-reticulum-resident kinase. *Nature* 397:271–274.
- Harding HP, Calton M, Urano F, Novoa I, Ron D (2002) Transcriptional and translational control in the mammalian unfolded protein response. *Annu Rev Cell Dev Biol* 18:575–599.
- Hille B (2001) Ion channels of excitable membranes, Ed 3. Sunderland, MA: Sinauer Associates.
- Iwashima Y, Abiko A, Ushikubi F, Hata A, Kaku K, Sano H, Eto M (2001) Downregulation of the voltage-dependent calcium channel (VDCC)  $\beta$ -subunit mRNAs in pancreatic islets of type 2 diabetic rats. *Biochem Biophys Res Commun* 280:923–932.
- Jones OT, Bernstein GM, Jones EJ, Jugloff DG, Law M, Wong W, Mills LR (1997) N-type calcium channels in the developing rat hippocampus: subunit, complex, and regional expression. *J Neurosci* 17:6152–6164.
- Kang MG, Campbell KP (2003)  $\gamma$  subunit of voltage-activated calcium channels. *J Biol Chem* 278:21315–21318.
- Kang MG, Chen CC, Felix R, Letts VA, Frankel WN, Mori Y, Campbell KP (2001) Biochemical and biophysical evidence for  $\gamma_2$  subunit association with neuronal voltage-activated Ca<sup>2+</sup> channels. *J Biol Chem* 276:32917–32924.
- Kim HL, Kim H, Lee P, King RG, Chin H (1992) Rat brain expresses an alternatively spliced form of the dihydropyridine-sensitive L-type Ca<sup>2+</sup> channel  $\alpha_2$  subunit. *Proc Natl Acad Sci USA* 89:3251–3255.
- Kleene R, Schachner M (2004) Glycans and neural cell interactions. *Nat Rev Neurosci* 5:195–208.
- Klugbauer N, Dai S, Specht V, Lacinova L, Marais E, Bohn G, Hofmann F (2000) A family of  $\gamma$ -like calcium channel subunits. *FEBS Lett* 470:189–197.
- Letts VA (2005) Stargazer—a mouse to seize! *Epilepsy Curr* 5:161–165.
- Letts VA, Felix R, Biddlecome GH, Arikath J, Mahaffey CL, Valenzuela A, Bartlett II FS, Mori Y, Campbell KP, Frankel WN (1998) The mouse stargazer gene encodes a neuronal Ca<sup>2+</sup>-channel  $\gamma$  subunit. *Nat Genet* 19:340–347.
- Letts VA, Kang MG, Mahaffey CL, Beyer B, Tenbrink H, Campbell KP, Frankel WN (2003) Phenotypic heterogeneity in the stargazin allelic series. *Mamm Genome* 14:506–513.
- Letts VA, Mahaffey CL, Beyer B, Frankel WN (2005) A targeted mutation in *Cacng4* exacerbates spike-wave seizures in stargazer (*Cacng2*) mice. *Proc Natl Acad Sci USA* 102:2123–2128.
- Lie AA, Blumcke I, Volsen SG, Wiestler OD, Elger CE, Beck H (1999) Distribution of voltage-dependent calcium channel  $\beta$  subunits in the hippocampus of patients with temporal lobe epilepsy. *Neuroscience* 93:449–456.
- Luo ZD, Chaplan SR, Higuera ES, Sorkin LS, Stauderman KA, Williams ME, Yaksh TL (2001) Upregulation of dorsal root ganglion  $\alpha_2\delta$  calcium channel subunit and its correlation with allodynia in spinal nerve-injured rats. *J Neurosci* 21:1868–1875.
- Marciniak SJ, Ron D (2006) Endoplasmic reticulum stress signaling in disease. *Physiol Rev* 86:1133–1149.
- Marty A, Neher E (1995) Tight-seal whole-cell recording. In: *Single-channel recording* (Sakmann B, Neher E, eds), pp 31–52. New York: Plenum.
- Moss FJ, Viard P, Davies A, Bertaso F, Page KM, Graham A, Canti C, Plumptre M, Plumptre C, Clare JJ, Dolphin AC (2002) The novel product of a five-exon stargazin-related gene abolishes Ca<sub>v</sub>2.2 calcium channel expression. *EMBO J* 21:1514–1523.
- Moss FJ, Dolphin AC, Clare JJ (2003) Human neuronal stargazin-like proteins,  $\gamma_2$ ,  $\gamma_3$  and  $\gamma_4$ ; an investigation of their specific localization in human brain and their influence on Ca<sub>v</sub>2.1 voltage-dependent calcium channels expressed in *Xenopus* oocytes. *BMC Neurosci* 4:23.
- Nyfelner B, Nufer O, Matsui T, Mori K, Hauri HP (2003) The cargo receptor ERGIC-53 is a target of the unfolded protein response. *Biochem Biophys Res Commun* 304:599–604.
- Page KM, Hebllich F, Davies A, Butcher AJ, Leroy J, Bertaso F, Pratt WS, Dolphin AC (2004) Dominant-negative calcium channel suppression by truncated constructs involves a kinase implicated in the unfolded protein response. *J Neurosci* 24:5400–5409.
- Price MG, Davis CF, Deng F, Burgess DL (2005) The alpha-amino-3-hydroxy-5-methyl-4-isoxazolepropionate receptor trafficking regulator “stargazin” is related to the claudin family of proteins by its ability to mediate cell-cell adhesion. *J Biol Chem* 280:19711–19720.
- Qiao X, Meng H (2003) Nonchannel functions of the calcium channel  $\gamma$  subunit: insight from research on the stargazer mutant. *J Bioenerg Biomembr* 35:661–670.
- Raghib A, Bertaso F, Davies A, Page KM, Meir A, Bogdanov Y, Dolphin AC (2001) Dominant-negative synthesis suppression of voltage-gated calcium channel Cav2.2 induced by truncated constructs. *J Neurosci* 21:8495–8504.
- Roussel M, Cens T, Restituito S, Barrere C, Black III JL, McEnery MW, Charney P (2001) Functional roles of  $\gamma_2$ ,  $\gamma_3$  and  $\gamma_4$ , three new Ca<sup>2+</sup> channel subunits, in P/Q-type Ca<sup>2+</sup> channel expressed in *Xenopus* oocytes. *J Physiol (Lond)* 532:583–593.
- Salceda E, Garateix A, Aneiros A, Salazar H, Lopez O, Soto E (2006) Effects of ApC, a sea anemone toxin, on sodium currents of mammalian neurons. *Brain Res* 1110:136–143.
- Sandoval A, Oviedo N, Andrade A, Felix R (2004) Glycosylation of asparagines 136 and 184 is necessary for the  $\alpha_2\delta$  subunit-mediated regulation of voltage-gated Ca<sup>2+</sup> channels. *FEBS Lett* 576:21–26.
- Vance CL, Begg CM, Lee WL, Haase H, Copeland TD, McEnery MW (1998) Differential expression and association of calcium channel  $\alpha_{1B}$  and  $\beta$  subunits during rat brain ontogeny. *J Biol Chem* 273:14495–14502.
- Zhou Y, Lee AS (1998) Mechanism for the suppression of the mammalian stress response by genistein, an anticancer phytoestrogen from soy. *J Natl Cancer Inst* 90:381–388.